ELSEVIER

Journal of Chromatography A, 740 (1996) 159–167

JOURNAL OF CHROMATOGRAPHY A

Packed-column hydrodynamic chromatography using 1-μm non-porous silica particles

E. Venema, J.C. Kraak, H. Poppe, R. Tijssen*

Laboratory for Analytical Chemistry, University of Amsterdam, Nieuwe Achtergracht 166, 1018 WV Amsterdam, The Netherlands

Received 15 December 1995; revised 8 February 1996; accepted 8 February 1996

Abstract

150×3 mm I.D. columns, packed with 1-μm non-porous spherical silica particles, were used to separate soluble synthetic polymers by hydrodynamic chromatography. The columns exhibited a plate height of about 1.4 μm allowing very fast and efficient separations of polymers in the molecular mass range 10^3–$2 \cdot 10^6$ g/mol. The migration behaviour of polymers could be well described by a simple theoretical model. The applicability of packed bed HDC for the fast separation of polymers was illustrated with separations of polystyrene and poly(methyl methacrylate) mixtures.

Keywords: Hydrodynamic chromatography; Packed columns, HDC; Column efficiency; Migration behaviour; Polymers; Polystyrene; Poly(methyl methacrylate)

1. Introduction

Synthetic polymers can be separated according to size using techniques such as size-exclusion chromatography (SEC) [1,2] and field-flow fractionation (FFF) [3,4].

A less known separation technique also capable to separate polymers according to size is packed column hydrodynamic chromatography (HDC) [5–7]. In this technique use is made of the parabolic flow profile as occurring in the interstitial space between the particles packed in a column. The separations are mainly due to the exclusion of solutes from the low velocity regions near the surface of the particles. A large polymer molecule will be more excluded from the low velocity regions near the wall than a smaller molecule. Consequently, the larger polymer will experience a higher mean solvent velocity and will be transported through the system faster than the mobile phase. Hence, the elution order is the same as in SEC, which has been confirmed by numerous experiments, both in packed and in open tubular columns [5–16].

The separation by HDC occurs only when the ratio between the size of the polymer and the flow channel, e.g., the aspect ratio, is not too small (>0.01).

At its introduction as a size separation technique in the 1970s, HDC was either performed in small-bore capillaries (I.D. 50–500 μm) or in columns packed with 10–20 μm particles.

In these systems the interstitial channels are relatively large, which restricts the application to very large solutes, such as fibres and solid particles [12–15].

The availability of fused-silica capillaries with internal diameters of 1–5 μm made it possible that

*Corresponding author.

0021-9673/96/$15.00
PII S0021-9673(96)00135-5

HDC entered the molecular mass range covered by SEC [8–11].

Using these capillaries, extremely small injection and detection volumes had to be used in order to prevent excessive peak broadening. Limitations in detection further required to inject highly concentrated samples, resulting in non-ideal behaviour of the system causing peak deformation. In order to circumvent the practical problems with capillaries, HDC on columns packed with 1.5-μm particles has been reported [16], thereby bringing the effective working range of HDC very close to that of SEC. As particle size determines the application range of HDC in terms of molecular mass or solute size, having small particle columns is an important issue. In the present paper, the successful preparation of 150×3 mm I.D. columns packed with 1-μm non-porous silica particles is reported. Extremely fast and efficient HDC separations of polymers on these columns will be shown.

2. Theory

2.1. Migration behaviour

Many theoretical models have been proposed to explain and predict the migration behaviour of polymers in HDC [7]. Most of these theories have been derived from the model as used to describe the migration of polymers in open capillaries [5,7–9]. In this model, the migration of a polymer is described by the quantity τ as function of λ, the aspect ratio, according to Ref. [8]:

$$\tau = \frac{t_p}{t_m} = \frac{1}{1 + 2\lambda - C\lambda^2} \quad (1)$$

where t_p is the migration time of a polymer, t_m the migration time of an infinite small sized marker, C is a constant accounting for secondary effects and ranges between 1 and 5 and λ is the aspect ratio, which is the ratio of the effective radius, R_{eff}, of the polymer and the radius of the capillary. It has been found that in packed bed HDC a C value of 2.7 describes the experimental migration behaviour of organic soluble polymers best [16]. Eq. (1) predicts that all polymers will elute in a migration window ranging from $0.73 \cdot V_0$ to V_0. Where V_0 is the elution volume of a small sized solute. The aspect ratio, λ, needed to predict the migration according to Eq. (1), can be calculated from the effective radius of the polymer and the channel width. The effective radius of a freely jointed chain polymer can be calculated as from the radius of gyration, R_g, by [17]:

$$R_{eff} = \frac{\sqrt{\pi}}{2} R_g \quad (2)$$

The radius of gyration can be found from lightscattering experiments and its dependence on the molecular mass of the polymer can be described generally by:

$$R_g = aM_w^b \quad (3)$$

where a and b are constants obtained from the lightscattering experiments and M_w is the molecular mass.

In open tubular HDC, the channel width is exactly known and equals the radius. In packed bed HDC, however, the radius of the interstitial channels is much harder to define.

In packed beds the capillary radius in Eq. (1) can be replaced by an effective radius by representing the interstitial channels as an array of cylindrical tubes with the same volume to surface ratio as the bed. In this way the effective channel radius, R_c, is found [7]:

$$R_c = \frac{d_p}{3} \frac{\epsilon}{1 - \epsilon} \quad (4)$$

where d_p is the particle diameter and ϵ the column porosity which is the ratio between the void volume of the packed column and the volume of the empty column.

The effective channel radius is derived from the hydraulic radius as used in chemical engineering and is equal to $2R_h$, where R_h is the hydraulic radius.

3. Dispersion

3.1. Peak dispersion

The peak capacity within the restricted migration window is strongly dependent on the efficiency of the column, e.g., the plate height.

In packed bed HDC it has been previously shown that the plate height can be well described by [19,20]:

$$H = \frac{B\,D_m}{\langle v \rangle} + \frac{d_p}{\left(\frac{D_m}{\langle v \rangle d_p} + \frac{1}{1.4}\right)} \quad (5)$$

where B is a constant and has a value of 1.2–1.4, D_m is the molecular diffusion coefficient, $<v>$ is the linear solvent velocity and d_p is the particle size. The first term in the equation describes the longitudinal diffusion of a component and the second term depicts the effect of convective mixing on the dispersion.

The longitudinal diffusion term is usually very small compared to the second term due to the low diffusion coefficient of polymers.

At higher solvent velocities the plate height will exhibit a constant value of around $1.4d_p$.

Eq. (5) only describes the peak broadening caused by the column. However, in practice, significant peak broadening can occur due to the polydispersity of the polymers and by external peak broadening caused by the injection, detection volumes and connecting tubing. These extra contributions will be discussed below.

3.2. Peak broadening by polydispersity

Often the polydispersity of the polymers in the sample is a major contributor to the observed peak broadening, not only in HDC but also in SEC and FFF. This makes it difficult to discriminate between the dispersion caused by the column and the peak broadening by polydispersity.

For SEC and FFF, the contribution of the polydispersity to the plate height, H_{pol}, can be estimated by [21,22]:

$$H_{pol} = L\,S^2(\mu - 1) \quad (6)$$

where L is the column length, S the mass-selectivity and μ the polydispersity of the sample, which is equal to the M_w/M_n ratio. Eq. (6) is only valid when the polydispersity of the polymer is below 1.05.

The mass-selectivity in Eq. (6) has been defined as follows [23]:

$$S = \left| \frac{d \ln R}{d \ln M_w} \right| \quad (7)$$

where R is the retention factor (t_0/t_r), equal to $1/\tau$.

By combining Eq. (1) and Eq. (7), the mass-selectivity for HDC can be written as:

$$S = b\frac{2\lambda(1 - C\lambda)}{1 + 2\lambda - C\lambda^2} = 2b\tau\lambda(1 - C\lambda) \quad (8)$$

where b is the same constant as in Eq. (3) and C is the same factor as in Eq. (1).

Fig. 1 shows the theoretical effect of the polydispersity on the observed plate height for a 15-cm long column packed with 1-μm particles for three polystyrene molecular masses.

It clearly shows that the apparent performance of the system can be reduced significantly by the polydispersity, in particular for the higher molecular masses and already at very small polydispersities.

One can find the plate height from experiments with polydisperse samples by extrapolating to zero column length [24], this is laborious and not applicable when the packing quality can differ with column length. Therefore, it is better to work with standards of sufficient small polydispersities or to use polymers with low molecular masses, so that polydispersity hardly plays a role in the observed efficiency. These latter methods were used to determine the column dispersion.

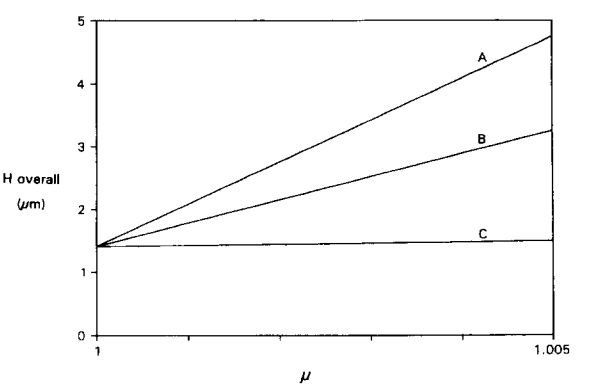

Fig. 1. Calculated contribution of the polydispersity to the overall plate height for PS (775 kDa, A) PS (336 kDa, B) and PS (12.5 kDa, C) in THF for a column packed with 1-μm particles.

3.3. External peak broadening effects

External peak broadening effects such as injection- and detection volume, frits and connecting tubing can significantly affect the performance. In order to minimize the external effects it is necessary to estimate the peak volumes of the eluting peaks.

For a Gaussian peak, the volume standard deviation, σ_v, of the peak in μl can be calculated by:

$$\sigma_v = V_r \sqrt{\frac{H}{L}} \tag{9}$$

where H is the plate height (μm), L the length of the column (μm) and V_r is the migration volume (μl).

Assuming that, in HDC, the plate height at higher solvent velocities reaches a constant value of $1.4d_p$, σ_v be expressed as:

$$\sigma_v = V_0 \tau \sqrt{\frac{1.4d_p}{L}} \tag{10}$$

where V_0 is the void volume of the column (μl).

Fig. 2 shows the σ_v of PS 500 kDa in THF for a 3 mm I.D. column as a function of the particle size. As can be seen, the volumes are around 1 μl. It can be expected that the use of a standard 8 μl UV detection cell, with a σ_v of at least 2.3 μl, will destroy the efficiency of the column. Therefore, in all experiments, special precautions were taken to minimize external peak broadening by using a detector cell with a small volume and keeping connecting tubing as short as possible.

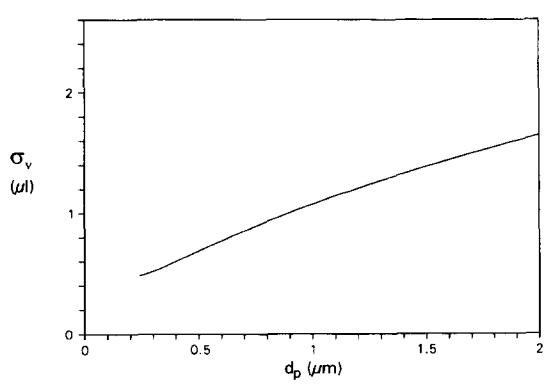

Fig. 2. Calculated effect of the particle diameter on σ_v of PS 500 kDa in THF in a 150×3 mm I.D. column.

4. Experimental

4.1. Materials

Analytical grade tetrahydrofuran (THF) and methanol were purchased from Janssen Chimica (Geel, Belgium). Prior to use, all solvents were filtered through a 0.02-μm inorganic filter (Anodisc 47, Anotec, Banbury, UK)

Polystyrene Polymer standards were obtained from Machery-Nagel (Düren, Germany), Merck (Darmstadt, Germany), Pressure Chemical (Pittsburgh, PA, USA) and Toyo Soda (Tokyo, Japan).

PMMA standards were purchased from Polymer Laboratories (Church Stretton, UK).

The silica particles were produced in our laboratory using the method of Unger [25]. The diameter of the particles was measured by electron microscopy and was found to be 0.998 μm ±2%.

The chromatographic system consisted of an HPLC pump (Spectroflow 400, ABI, Ramsey, NJ, USA) operated at flow-rates between 0.17 and 0.87 ml/min, a variable-wavelength UV detector (Spectroflow 757, ABI, Ramsey, NJ, USA) or an evaporative light scattering detector (ELSD IIA, Varex, Burtonsville, MD, USA).

Injections were made using a valve with an internal loop of 1 μl (7413, Rheodyne, Cotati, CA, USA). The detector signal was monitored using a recorder (BD 40, Kipp en Zonen, Delft, Netherlands) and an integrator (3390A, Hewlett-Packard, Avondale, PA, USA).

4.2. Injection and detection

As was stated in the theoretical part, special attention has to be paid to the injection and detection in order to prevent excessive external peak broadening.

It was found necessary to use a split injection, with a split ratio of 1 to 4, to minimize the dispersion. In Fig. 3 the split injection set-up is schematically represented.

Also the UV-detection cell volume had to be

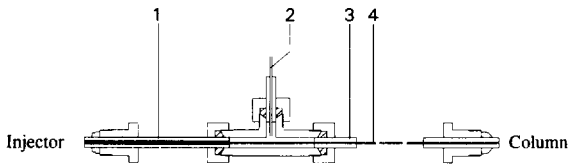

Fig. 3. Schematic representation of the split injection. (1) stainless-steel tubing; (2) restriction capillary; (3) PEEK 0.5 mm I.D.; (4) fused-silica capillary, 370 μm O.D., 75 μm I.D., length 12 cm.

decreased drastically and this was realized by replacing the standard 8-μl cell by a capillary slit cell where detection takes place through a 75 μm capillary connected to the column outlet [26]. In order to minimize the external peak broadening with the ELSD, the original stainless steel tubing to connect the column with the detector was replaced by a 12 cm×75 μm I.D. fused-silica capillary.

4.3. Column preparation

The columns used were made of 316 stainless steel with the dimensions of 150×3 mm I.D.. Initially standard 0.5-μm stainless steel frits were used in the end fittings. However, it appears that these frits caused a large peak broadening. Therefore we constructed a home-made frit consisting of a 0.5-μm filter (Type FH, Millipore, Bedford, MA, USA) sandwiched between two 10-μm steel screens (Vici, Schenkon, Switzerland). The thickness of the complete frit was about 0.3 mm. Columns were packed by the slurry technique with methanol as the slurry and packing liquid [16]. The slurry was made by suspending 2.5 g silica in 25 ml methanol. After sonicating for 20 min, the remaining agglomerates were removed by filtering the slurry through a 10 μm steel filter (Vici). Prior to packing, the solution was sonicated for another 20 min.

During packing the pressure was increased to 980 bar in 2 min. At this final pressure 50 ml of methanol was flushed through the column. After the pump was switched off the pressure was allowed to drop to zero in about 1 h before the column was disconnected.

After installing the end fitting the column was connected to the chromatographic system and was flushed with THF until a steady detector signal was obtained.

4.4. Sample preparation and injection

The polymer sample solutions were prepared at a concentration of 0.1 mg/ml in THF. After adding THF the samples were left overnight to swell and dissolve slowly. To samples with molecular masses >97.2 kDa, a marker, PS 580, was added. For the samples containing molecular masses <97.2 kDa, no marker was added because the peaks of the polymer and marker overlap. In these cases the marker was separately injected about 30 s after the injection of polymer solution. All measurements were performed in triplicate to obtain accurate average values.

5. Results

5.1. Column characteristics

For the calculation of the effective channel radius of the packed bed, the column porosity, ϵ, has to be known. The void volume was measured in two ways: by injecting a small sized marker at a specific flow-rate and from the weighing of the column using two different solvents [26]. In both cases the column porosity was found to be 0.391.

Using Eq. (4), the effective channel radius for the 1-μm particles was then calculated to be 0.213 μm.

The column resistance, φ, of a packed bed gives information on how well the column is packed and can be calculated by:

$$\varphi = \Delta P \frac{d_p^2}{\langle v \rangle \eta L} \tag{11}$$

where η is the viscosity of the solvent (Pa s), $<v>$ is the linear solvent velocity (mm/s), d_p is the particle diameter (mm), L is the column length (mm) and ΔP is the observed pressure drop (Pa).

The column packed with the 1-μm particles had a φ value of 382. For columns packed with non-porous particles a φ value of about 400 is considered as normal [26]. Therefore it can be assumed that the column is well packed.

5.2. Column efficiency

The efficiency of the column was determined by measuring the plate height as a function of the

solvent velocity with two PS solutes, PS 12.5 kDa and PS 775 kDa.

The plate height was calculated according to:

$$H = \frac{\sigma_t^2 L}{t_r^2} \tag{12}$$

where L is the length of the column (μm), t_r the migration time (s) and σ_t standard deviation of the peak (s) measured at 0.607 times the peak height.

From these measurements a plate-height curve was constructed as shown in Fig. 4. For PS 12.5 kDa the plate height decreases with increasing solvent velocity and approaches a constant value at the higher velocities. The higher plate height for PS 12.5 kDa at the low solvent velocities can be attributed to broadening by molecular diffusion. For PS 775 kDa an increase in plate height is not observed because the diffusion coefficient is much smaller than for PS 12.5 kDa. Therefore molecular diffusion hardly plays a role in the observed efficiency and a constant plate height of 1.4 μm was found over the entire velocity region, which corresponds to the expected minium plate height according to Eq. (5).

The presented plate heights include possible broadening effects due to the polydispersity.

In the theoretical part it was already mentioned that polydispersity can play a dominant role in the extent of peak broadening in chromatographic polymer analysis techniques. This complicates the interpretation of efficiency data because the peak broadening caused by the column cannot easily be separated from the broadening caused by the polymer.

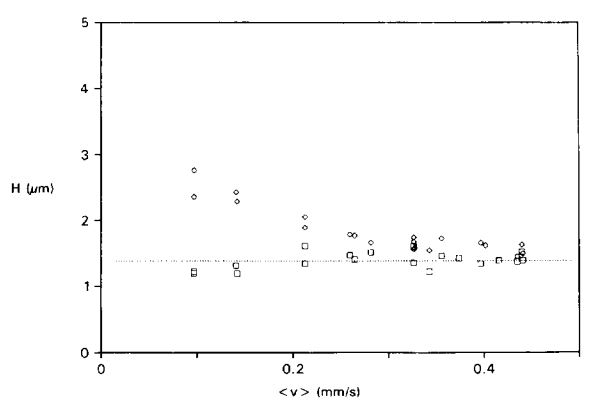

Fig. 4. Plate height (H) versus linear velocity ($<v>$) for PS in THF. Dashed line, theoretical minimum value, (□) PS 775 kDa, (◇) PS 12.5 kDa.

In the case of PS 775 kDa the manufacturer stated a polydispersity of 1.01. According to Eq. (6) this should give a plate height of about 10 μm. This value is seven times larger than was experimentally observed. Even when the total observed dispersion is fully attributed to polydispersity, a M_w/M_n ratio is found of 1.0014. It is clear that the true polydispersity must be even significantly lower. This discrepancy between the polydispersity as stated by the manufacturer and as measured has been observed before [19,21].

6. Migration behaviour

6.1. Polystyrene

The effective radius, R_{eff}, of a polymer molecule has to be known in order to construct a calibration curve. The effective radius can be calculated from the radius of gyration according to Eq. (3). For polystyrene the radius of gyration, according to Eq. (2), in THF has been determined by light scattering and can be calculated as in Ref. [27]:

$$R_g = 1.39 \cdot 10^{-5} M_w^{0.588} \tag{13}$$

where R_g is the radius of gyration (μm) and M_w is the weight-average molecular mass (g/mol).

Fig. 5 shows the experimental and theoretical migration behaviour of PS standards at three different solvent velocities. The reversal of the theoretical curve in Fig. 5 at higher molecular mass can be attributed to the extent to which the centre of mass of a polymer lags the eluent velocity [7–9,16,29].

As can be seen, the τ values are independent of the solvent velocity up to a molecular mass of 1260 kDa, but for the higher masses the experimental points clearly deviate from the theoretical line. This deviation has been observed before and can be attributed to polymer deformation [18]. Polymer elongation, caused by shear deformation, will decrease the effective radius of the polymer and thus results in larger τ values.

Polymer degradation, which could also cause a

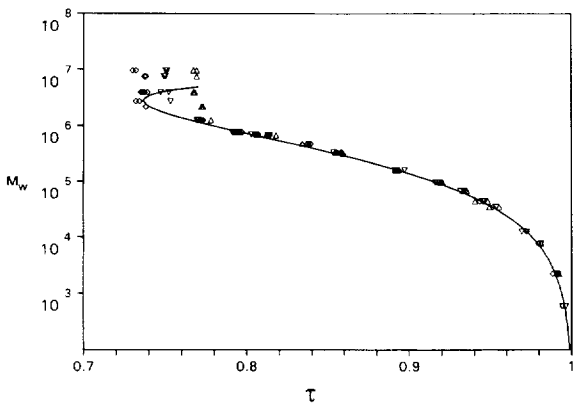

Fig. 5. Theoretical calibration curve (solid line) and experimental results for polystyrene in THF. Solvent velocity: (◊) 0.28 mm/s; $\Delta P = 95$ bar, (▽) 0.56 mm/s; $\Delta P = 200$ bar and (△) 0.87 mm/s; $\Delta P = 335$ bar.

shift in retention can be ruled out. First of all, no increase in baseline is observed which could indicate the fragmentation of polymers. Also, investigations by other workers [16] showed that even at high flow-rates no polymer degradation occurred.

The occurrence of polymer deformation can be predicted from the Deborah number which can be calculated according to Ref. [29]:

$$\mathrm{Deb} = K\frac{\epsilon v}{d_p}\frac{6.12\phi\eta R_g^3}{RT} \qquad (14)$$

where K is a constant with a value around 6, ϕ is the Flory–Fox parameter (ca. $2.5\cdot10^{23}$ mol^{-1}), η is the solvent viscosity, R_g is the radius of gyration of the polymer, R is the gas constant and T is the absolute temperature.

Above a Deborah number of 0.1 it is assumed that polymer deformation can occur.

In Table 1 the calculated Deborah numbers and the experimental τ values, as a function of the solvent velocity, are given for polymers with molecular masses over 775 kDa.

Up to a molecular mass of 1260 kDa, the τ values are independent of the solvent velocity. This would imply that no deformation of these polymers occurs, in agreement with calculated Deborah numbers below 0.1. However, for molecular masses above 1260 kDa the τ values increase significantly with increasing solvent velocity. This behaviour and the fact that the Deborah numbers are well over 0.1 indicates the occurrence of polymer deformation.

Surprisingly, the τ values of the larger polymers are almost equal for a given velocity. This finding might indicate that the large polymers migrate through the packing more or less as a sausage. Also lift forces might be responsible for the observed behaviour.

For the column packed with 1-μm particles, HDC appears to be best suitable to PS in the molecular mass range of 10^3–$2\cdot10^6$ g/mol.

6.2. Poly(methyl methacrylate)

PMMA has no UV-chromophor and therefore, the evaporative light scattering detector (ELSD) had to be used. A disadvantage of the ELSD is the peak sharpening [28,29] due to the non-linear calibration line. Calculated plate heights from ELSD measurements must be corrected for this effect to prevent an exaggeration of the system performance. In this case,

Table 1
Theoretical calculated Deborah numbers and experimental τ values for PS standards in THF at different solvent velocities

Molecular mass (kDa)	$<v>$ (mm/s)					
	0.28		0.56		0.87	
	Deb	τ	Deb	τ	Deb	τ
9800	0.738	0.731	1.477	0.751	2.294	0.768
7700	0.482	0.737	0.965	0.750	1.499	0.769
4000	0.152	0.738	0.304	0.747	0.472	0.768
2750	0.078	0.733	0.157	0.753	0.244	0.773
1260	0.020	0.773	0.040	0.769	0.062	0.770
775	0.008	0.794	0.014	0.793	0.026	0.795

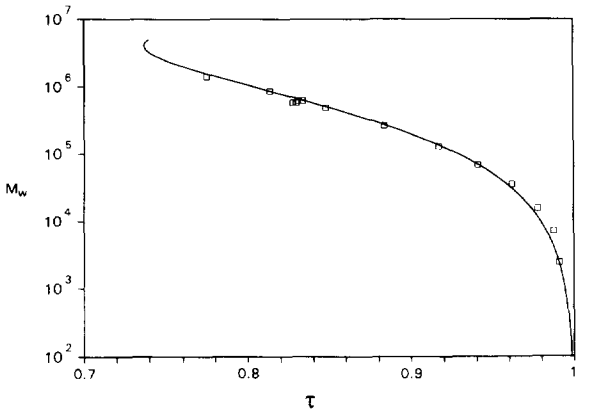

Fig. 6. Theoretical calibration curve (solid line) and experimental results (□) for poly(methyl methacrylate) in THF, $<v>$ =0.28 mm/s; ΔP=95 bar.

correction was not necessary because PMMA was not used to calculate plate heights for this column.

For PMMA in THF, also, a direct relationship between molecular mass and radius of gyration is available [30]:

$$R_g = 1.2 \cdot 10^{-5} M_w^{0.583} \quad (15)$$

Due to the limited number of samples with different molecular masses available it was not possible to construct a complete calibration curve. Fig. 6 shows the experimental points and the theoretically line at a solvent velocity of 0.28 mm/s.

As can be seen, the experimental and theoretical data are in good agreement.

7. Separations

The separation power and high speed of the column packed with 1-μm particles is demonstrated in Fig. 7 and Fig. 8. Fig. 7 shows an efficient separation of a mixture of ten PS molecular masses ranging from 2.2 to 2200 kDa. As can be seen, HDC is a very fast separation technique allowing the separation of this PS mixture in less then 5 min. Similar results were obtained with a PMMA solutions using the ELSD as can be seen in Fig. 8. In both chromatograms a small increase in base line signal, before the first eluting peak, can be noticed.

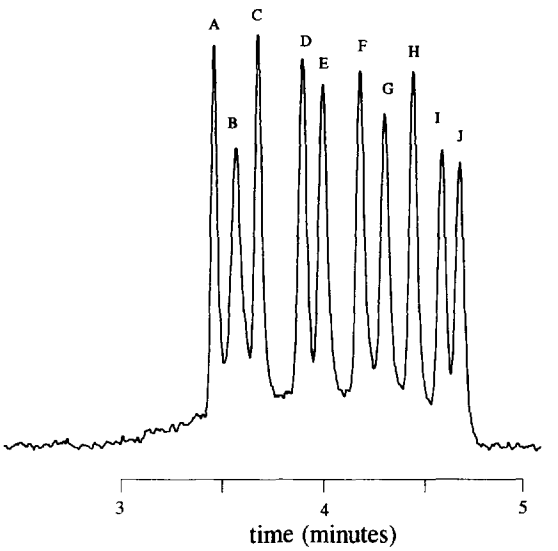

Fig. 7. Separation of a mixture of polystyrenes in THF by HDC. solvent speed, 0.56 mm/s; detection, UV, 210 nm; solutes, (A) PS 2200 kDa, (B) PS 1260 kDa, (C) PS 775 kDa, (D) PS 475 kDa, (E) PS 336 kDa, (F) PS 160 kDa, (G) PS 97.2 kDa, (H) PS 43.9 kDa, (I) PS 12.5 kDa, (J) PS 2.2 kDa.

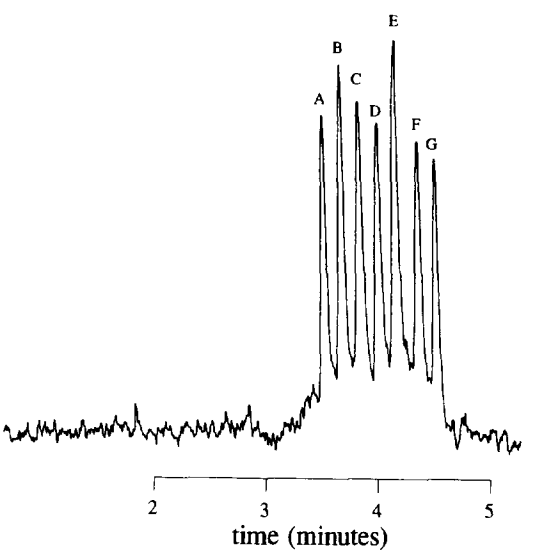

Fig. 8. Separation of a mixture of poly(methyl methacrylates) in THF by HDC. Column and solvent speed as in figure 7; Detection, ELSD; Solutes, (A) PMMA 1 400 kDa, (B) PMMA 840 kDa, (C) PMMA 470 kDa, (D) PMMA 260 kDa, (E) PMMA 127 kDa, (F) PMMA 34.5 kDa, (G) PMMA 2.4 kDa.

This increase is most probably due to the high viscosity of the sample. When more concentrated samples are injected the increase becomes more pronounced.

From these figures it can be seen that packed column HDC with 1-μm non-porous silica particles is a very efficient and fast technique for the separation of polymers according to size. Especially the high speed can be useful when HDC is used in a two dimensional separation technique such as FFF–HDC.

8. Conclusions

Very efficient columns can be packed with 1-μm non-porous spherical silica particles. By keeping the external peak broadening small, on 150×3 mm columns more than 110 000 plates can be generated. The columns are extremely suited to realize very fast separations of soluble polymers in the molecular mass range 10^3–$2 \cdot 10^6$ g/mol by HDC thereby covering the same range as in SEC. The migration of PS and PMMA on the column fits perfectly with the theoretical HDC model. The separation speed of HDC with 1-μm particles makes the technique an attractive alternative to SEC.

Also the speed of HDC makes it an appealing method to use in multi dimensional system such as FFF–HDC.

Acknowledgments

This research was supported by Shell Research B.V. (Amsterdam, The Netherlands).

References

[1] W.W. Yau, J.J. Kirkland, D.D. Bly, Modern Size-Exclusion Liquid Chromatography, Wiley-Interscience, New York, NY, 1979.
[2] J.H. Knox, H.P. Scott, J. Chromatogr., 316 (1984) 333.
[3] J.C. Giddings, Sep. Sci., 1 (1966) 123.
[4] J.C. Giddings, Science, 260 (1993) 1456.
[5] E.A. DiMarzio, C.M. Guttmann, Macromolecules, 2 (1970) 131.
[6] H.J. Small, J. Colloid Interface Sci., 48 (1974) 147.
[7] A.J. McHugh, CRC Crit. Rev. Anal. Chem., 15 (1984) 63.
[8] R. Tijssen, J. Bos, M.E. van Kreveld, Anal. Chem., 58 (1986) 3036.
[9] C.A. Silebi, J.G. DosRamos, J. Colloid Interface Sci., 130 (1989) 14.
[10] J. Bos, R. Tijssen, M.E. van Kreveld, Anal. Chem., 61 (1989) 1318.
[11] J.G. DosRamos, C.A. Silebi, Polym. Int., 30 (1993) 445.
[12] H. Small, F.L. Saunders, J. Sale, Adv. Colloid Interface Sci., 6 (1976) 237.
[13] E.A. Silebi, A.J. McHugh, Am. Inst. Chem. Eng. J., 24 (1978) 204.
[14] B.A. Buffham, J. Colloid Interface Sci., 67 (1978) 154.
[15] R.F. Stoisits, G.W. Poehlein, J.W. Vanderhoff, J. Colloid Interface Sci., 57 (1976) 337.
[16] G. Stegeman, J.C. Kraak, H. Poppe, R. Tijssen, J. Chromatogr. A, 657 (1993) 283.
[17] M.E. van Kreveld, N. van den Hoed, J. Chromatogr., 83 (1973) 111.
[18] D.A. Hoagland, R.K. Prud'homme, Macromolecules, 22 (1989) 775.
[19] G. Stegeman, J.C. Kraak, H. Poppe, J. Chromatogr., 634 (1993) 149.
[20] J.C. Giddings, L.M.Jr. Bowman, M.N. Myers, Macromolecules, 2 (1977) 443.
[21] M.E. Schimpf, M.N. Myers, J.C. Giddings, J. Appl. Polym. Sci., 33 (1987) 117.
[22] J.H. Knox, F. McLennan, Chromatographia, 10 (1977) 75.
[23] J.C. Giddings, M.N. Myers, J. Janča, J. Chromatogr., 186 (1979) 37.
[24] J.H. Knox, F. McLennan, J. Chromatogr., 185 (1979) 289.
[25] K.K Unger, H. Giesche, German Patent DE-3534 143.2 (1985).
[26] G. Stegeman, R. Oostervink, J.C. Kraak, H. Poppe, K.K. Unger, J. Chromatogr., 506 (1990) 547.
[27] G.V. Schulz, H. Baumann, Makromol. Chem., 114 (1968), 122.
[28] A. Stolyhwo, H. Colin, M. Martin, G. Guiochon, J. Chromatogr., 288 (1984) 253.
[29] A. Stolyhwo, H. Colin, G. Guiochon, J. Chromatogr., 265 (1983) 1.
[30] S. Podzimek, 4 (1960) 1020, J. Appl. Polym. Sci., 54 (1994) 91.